HSPC The Open Access Publisher

JCCM ISSN 2575-0143 JOURNAL OF CARDIOLOGY AND CARDIOVASCULAR MEDICINE

Review Article

A mouse model of coronary microvacsular disease using a photochemical approach

Xinlu Wang[1-3], Fang Liu[1,2] and Zhen W. Zhuang[1,2,4]*

[1]Section of Cardiovascular Medicine, Yale University School of Medicine, New Haven, Connecticut, USA
[2]Yale Cardiovascular Research Center, Department of Internal Medicine, New Haven, USA
[3]Department of Ultrasound, Sheng Jing Hospital of China Medical University, Shenyang 110004, P.R. China
[4]Yale Translational Research Imaging Center, Yale University School of Medicine, New Haven, Connecticut, USA

Abstract

The development of reproducible rodent models of coronary microvascular disease (MVD) is essential for the early detection, treatment, and mechanism study of the pathophysiology. We hypothesized that endothelial dysfunction and subsequent microthrombi in the coronary arterioles, two early events in clinical coronary MVD, could be reproduced by photochemical reaction (PCR) technology in mice hearts. After rose bengal (one of photosensitizers) was administrated systemically, a green light was locally used to activate the photosensitizer, inducing over-production of oxidative stress in the heart. Following PCR, animals demonstrated reproducible endothelial injury, occlusion in arterioles, focal ischemia, and infarct-let with preserved cardiac function. Our technique has proven to be a reliable and reproducible means of creating coronary MVD in mice. We believe that this is an ideal model for developing a novel molecular tracer for earlier detection of coronary MVD, for testing new anti-fibrinolytic drugs, and for investigating the complex pathophysiology of coronary MVD. The protocol for establishing this model takes about thirty to forty minutes.

More Information

***Address for Correspondence:** Zhen W. Zhuang, Section of Cardiovascular Medicine, Yale University School of Medicine, New Haven, Connecticut, USA, Tel: 203-231-9084; Email: zwz2@connect.yale.edu

Submitted: 06 September 2019
Approved: 17 September 2019
Published: 18 September 2019

How to cite this article: Wang X, Liu F, Zhuang ZW. A mouse model of coronary microvacsular disease using a photochemical approach. J Cardiol Cardiovasc Med. 2019; 4: 120-130.

DOI: dx.doi.org/10.29328/journal.jccm.1001052

ORCID ID: orcid.org/0000-0001-5817-5549

Introduction

Every year, more than eight million patients in the USA alone visit the emergency department with complaints of chest pain. Nearly 70% of these patients are diagnosed with unexplained chest pain (UCP). Results from the NIH-WISE (Women's Ischemia Syndrome Evaluation) study indicated that as many as three million American women and one million men actually suffer from coronary microvascular disease (MVD), with an estimated 100,000 new cases occurring annually [1-3]. This disease was first reported in pre-menopausal women, who complained about atypical chest pain, but had normal cardiac function and coronary angiogram [4]. The current diagnosis of MVD is one of exclusion in the emergency department. Endomyocardial biopsies in these patients found endothelial injury, hypertrophy of the arteriolar media, marked perivascular fibrosis, and narrowing arteriole luminal without significant stenosis in the epicardial coronary artery [5,6]. For early diagnosis and possible prevention of disease progress, we hypothesize that endothelial dysfunction and possible microthrombi in the coronary arterioles, two early events in clinical coronary MVD, could be reproduced by photochemical reaction (PCR) technology in mice hearts [7].

Clustering of risk factors, such as obesity, hypercholesterolemia, hypertension, diabetes, and metabolic syndromes, may be responsible for MVD [8]. These factors have been associated with coronary micro- and macro-vascular dysfunction [2,9-12]. The mechanisms underlying endothelial dysfunction include enhanced superoxide production in endothelial cells (ECs) mediated by NADPH oxidase [8], and a reduction of nitric oxide (NO) [13]. Impairment of endothelium-mediated vasodilatation has been demonstrated in patients with MVD, and was prevented by the administration of L-arginine [14]. A substantial body of evidence attributes reactive oxygen species (ROS) as an early event for endothelial dysfunction and coronary disease progression [15,16]. NADPH oxidase family has been identified as major sources of these ROS [17]. Oxidative stress occurs when an imbalance develops between the production of ROS and the efficacy of the cell's anti-oxidant defense, leading to an altered redox status [18].

ROS have been shown to be involved in collagen-induced platelet activation and aggregation [19], and thrombin-induced vasoconstriction [20]. Both processes facilitate micro-thrombogenesis and consequent myocardial ischemia. The exact mechanism (pathogenesis) of coronary MVD, however, remains uncertain. Furthermore, there is no specific treatment for this disease.

Thus, the development of reproducible rodent models of coronary MVD is essential for the study of the pathophysiology, early detection, and therapy. Animal models of human diseases are a source of great insight, yet they also carry potentially crucial limitations that may confound experimental data [21].

Useful models should incorporate the following essential features: (i) mimic natural events in the human body, (ii) low cost, (iii) small animal size, and (iv) maintain a provision for sufficient materials for the study of cellular and molecular mechanisms. Rodents, especially murine, meet these requirements, which ensure their popularity for models of vascular diseases. More importantly, the broad availability of genetically modified mice strains increases the potential to discover the role of particular genes in the pathophysiology of coronary MVD.

Current experimental models of coronary MVD

Rodent and pig models of coronary thrombosis or thrombo-embolization have been studied in the past. Nichols, et al. combined balloon catheter injury with external compression to induce coronary thrombosis at the site of stenosis [22]. This procedure consistently exposed the media and induced platelet–fibrin micro-thrombi in normal pigs. Additionally, instead of an *in situ* primary thrombosis model, a micro-embolization model was developed by injecting different sized microspheres into the coronary arteries of large animals to mimic human MVD [23-26]. Unfortunately, the microspheres were chemically inert and were not chemo-attractants. Thus, this model only reproduces the physical obstruction without the endothelial dysfunction or injury and inflammatory response, both important components for a biologically relevant model. Recently, a homologous thrombotic model was used to create coronary micro-embolization in rats, where the expression of inflammatory cytokines and left ventricular dysfunction was reported [27]. Intravenous norepinephrine can also induce micro-embolization by platelet aggregation and subsequent micro-infarction, but it is limited to only large animal models [28]. A myocardial cryo-injury model was also recently been described [29,30], however, there are no consistent results. In our laboratory, we have successfully adopted photochemical reaction (PCR) technology to induce coronary MVD in mice [7]. We believe that damaged endothelium and subsequent micro-thrombi with physical and bioactive properties provide the much-needed model to study disease process. Therefore, this model can be used in further studies on the pathophysiology of coronary MVD, for the development of a novel imaging technique for early detection [7], and for the evaluation of anti-thrombotic or anti-fibrinolytic drugs.

Advantages and limitations of our model

The key advantages of our model are as follows:

- Animal preparation is relative simple without surgical or mechanical manipulation of the coronary artery or myocardium.
- *In situ* micro-thrombosis occludes coronary arterioles at the site where focal PCR is applied, maintaining patent conduct coronary artery and normal downstream microvasculature (not thrombo-embolization model). Thus, the affected myocardium is well confined within the territory illuminated by PCR, leading to predicable and reproducible focal myocardial ischemia and infarct-let. Spontaneous recanalization of the occluded arterioles doesn't occur at 24 hours or later.
- Lesion size and location are highly reproducible.
- Lesion sizes can be modulated by altering the illumination intensities, exposed durations of green light, beam positions, and photosensitizer concentrations. With longer illumination period, a large ischemic lesion with conduct coronary spasms can be induced.
- The procedure-associated mortality rate is low (<6%).
- Animals exhibit preserved global cardiac function.
- Photo-thrombotic MVD allows long-term survival.

The main limitation of our model is the establishment of an epicardial MVD lesion, which is different from clinical lesions (mainly in the endocardial region).

Experimental Design

The protocol contains three modules that allow a user to (1) establish a rodent model of coronary MVD, (2) investigate the preservation of cardiac function with cardiac-gated micro-CT, and (3) evaluate the occlusion of the coronary arterioles (rarefaction of coronary arterioles) and the patency of the conduct coronary at early stages using high-resolution coronary micro-CT angiograms.

Animals

The model damages coronary microvasculature in adult mice and requires a fully developed coronary system. Therefore, mice, aged 8-12 weeks, are used in this study. In our laboratory, only female mice are used because 70% of clinical coronary MVD predominantly occurs in females. The number of mice needed depends on laboratory experience, genetic background, and phenotype. Given that the user is well trained in microscopic rodent surgeries, for most users, 8-12 animals per group should be enough to gain statistically reliable data. The presented MVD model is suitable for all mice strains, as there is only minimal variation in the gross vascular anatomy of the coronary artery and its main branches.

Surgery

We provide a protocol to study coronary MVD, including ROS-induced endothelial injury and microthrombi at early stages, and infarct-let and peri-arteriole fibrosis at late stages. In the same mouse, cardiac function can subsequently be analyzed based on *in vivo* cardiac gated CT angiogram. To develop rodent models of coronary MVD, it is critical to induce *in situ* microthrombi, not embo-thrombosis from blood upstream. During surgery, it is important not to injure the main coronary artery or sinus vein due to the presence of epicardial spasm (stenosis), which may result in a baseline reduction of microvascular resistance, known to directly influence the development of coronary MVD. The minimum achievable microvascular resistance increases proportionally with the severity of an epicardial artery stenosis. We therefore exclude mice with trauma or occlusion of the sinus vein from the study.

Preparation of fresh photosensitizer (Figure 1a-b)

The formation of *in situ* ROS overproduction and subsequent micro-thrombi in the coronary arterioles is an essential step for the induction of a reproducible MVD model. The two primary components of PCR include a proper concentration of a specific photosensitizer (rose bengal in this study) and a matched wave-length light (low energy green light with wavelength 540 nm). Their interaction determines the ROS production, although individually they are harmless. Rose bengal initially absorbs photons from light, excites to the singlet state, and then relaxes to the longer-lived triplet state. Finally, two reactions happen under molecular oxygen: type 1 reaction leads to the formation of reactive oxygen species (ROS) and type 2 leads to singlet oxygen [31]. Based on our study, 10% rose bengal in saline and 4-minute illumination should be used to induce primary endothelial cells injury, not apoptosis, both *in vitro* and *in vivo* [7].

Preparation of sterile extension of illumination (Figure 1d-e)

To facilitate the delivery of the specific wave-length green light onto the small targeted area in the territory of the left anterior descending (LAD) artery, a light guide extension with a 2 mm-diameter tip and 30 mm in length is made with a sterilized filter tip of the pipet (200 μm) for original flexible light guide 1500ECO (4.5 mm diameter & 800 mm length, Figure 1c), which permits easy access to the surface of the heart.

PCR-induced coronary MVD

To induce coronary MVD, it is crucial to activate rose bengal locally in the arterioles level, which makes small lesions possible and improves survival rate by maintaining the conduct coronary and its distal downstream microvasculature patent (out of the illuminated zone). The procedures that we describe herein are based on our extensive experience

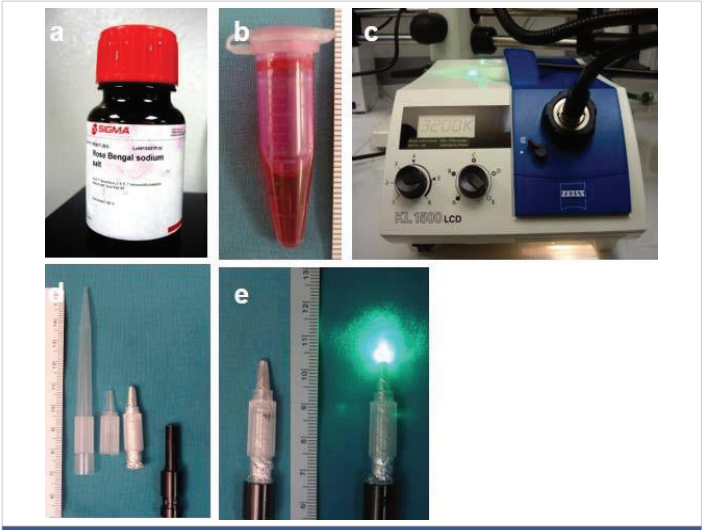

Figure 1: Photochemical reaction setup. (a) Rose bengal powder from Sigma. (b) 10 mg/ml rose bengal solution. (c) KL1500 LCD cold light source with flexible light guide 1500ECO (4.5 mm diameter & 800 mm length) and green light filter inside. (d) Home-made light guide extension with 2 mm diameter tip and 30mm in length to facilitate the delivery of light onto the small targeted area. (e) Extension on the distal light guide with power off and on.

using female wild-type mice, in which the LAD coronary is not directly visible after thoracotomy, and in which coronary sinus branches are used as land-markers. Thus, focal PCR can be induced for 4-minutes' illumination locally, 1-minute after administration of rose bengal. For the control, mice are subjected to an identical surgical procedure, but rose bengal is not injected (light only), or light is not delivered (photosensitizer only), or neither of the two are used. Although the procedures are primarily developed for young adult mice, these procedures are highly adaptable to other strains of mice, including transgenic or knockout mouse and aged rodents. This is achieved by adjusting the illumination time, the size of the tip of illumination, and the concentration of rose bengal.

Materials

Reagents

Experimental animals: Eight to twelve weeks old C57BL/6J female mice weighing 20-25 g (Charles River Laboratories) are used. These young female mice are selected due to the high frequency of coronary MVD occurring primarily in young women in the clinical setting.

! CAUTION: All animal requisitions, housing, procedures and imaging must comply with all federal, state and institutional laws, guidelines and regulations. The protocol described here (Protocol No: 2014-11429) has been reviewed by Yale University Institutional Animal Care and Use Committee and followed all federal and state guidelines concerning the use of animals in research and teaching, as defined by the Guide for the Care and Use of Laboratory Animals.

Isothesia (Isoflurane USP), 250 ml (Butler Schen Animal Healthcare), NDC. 11695-6776-2, http://www.butlerschein.com/).

! CAUTION: Anesthetic agent, causes central nervous system depression. Avoid exposure to vapors.

Puralube Vet Ointment (Dechra Veterinary Products, NDC: 17033-211-38) Nair hair removing cream (Church & Dwight Co, Inc. Ewing, NJ)

Betadine (Purdue Products LP, NDC: 67618-151-17)

Sterile alcohol prep pads (Fisher Healthcare, CN: 06-669-62).

Rose bengal sodium salt (Sigma Aldrich, cat No 632-69-9, http://www.sigmaaldrich.com/united- states.html)

Sodium chloride (0.9% (wt/vol)), 10ml (APP Pharmaceuticals, NDC 63323-186-10, http://www.apppharma.com/)

Buprenex, 0.3 mg vial (Reckitt Benckiser Pharmaceuticals Inc, cat. no. 924601, a DEA Schedule III controlled drug)

Cephalexan, 1 gram (WG Critical Care LLC, Paramus NJ, NDC: 44567-7-7-25)

eXia™ 160 (160 mgI/ml, Binitio Biomedical Inc, Ottawa, Ontario, Canada)

Heparin, 1,000 Units/ ml, 30 ml (APP Pharmaceuticals, NDC 63323-540-31, http://www.apppharma.com/)

Bismuth Oxychloride (Aldrich Chemistry)

Paraformaldehyde (MP Biomedicals, LLC, cat no. 0215014601 http://www.mpbio.com/US).

Equipment

Germinator 500™ glass bead sterilizer (Roboz, Gaithersbrug, MD, http://www.roboz.com/): This equipment uses 1.5 mm lead free glass beads to quickly decontaminate metal instruments between procedures. The unique heated glass bead bath remains at a constant 500°F, allowing the tips of instruments to be decontaminated within 15 seconds. High-temperature sterilizing autoclaves can be used as an alternative.

! CAUTION: This equipment operates at high temperatures. Do not touch the glass beads when hot.

Surgical instruments (Fine Science Tools (USA), Inc, Foster City): razor, micro-dissection scissors, Dumont straight and curved tip serrated forceps, thinner tipped forceps, needle holder and dissector, stitching set, blunt scissors, hemostat, iridectomy scissors.

TP-500 Heat Therapy Pump (Gaymar Industries Inc., Orchard Park, NY) with 31/3.5" x 23" C series pad.

Styrofoam pad (23 cm x 18 cm) with a heating pad on the top (Figure 2c): this is used to facilitate fixation of the muscle retractors while retaining maximum flexibility in positioning the mouse.

Anesthesia system includes a high-pressure supply of oxygen gases, pressure gauges, flowmeters, metal vaporizer (Smith Medical, Waukesha, WI), and breathing system (three-way stopcock & mouth mask).

! CAUTION: Each of these should be switched on or off with a three- way to allow isoflurane inhalant to be administered to animals during surgery (Figure 2a-c).

Compressed oxygen cylinder, USP grade (Airgas, cat. no. OX USP200, http://www.airgas.com/)

Intubation cannula with luer adapter (Harvard Apparatus)

Harvard rodent ventilator (model 687; Harvard Apparatus)

Leica MI6 stereo microscope (Leica, http://www.leica-microsystems.com/)

Polyethylene tubing PE10, (inner diameter 0.28 mm, outer diameter 0.61 mm; Becton Dickson and company, No. 427401)

Cotton-tipped applicators (Puritan, Hardwood Products Company)

Insulin Syringe with 29G needle (3/10 ml; Terumor Medical corporation)

Latex gloves (Microflex corporation)

25G needle (Becton Dickinson and Company)

Medi-pak™ surgical cautery (Mckesson Corporation)

Home-made muscle retractor: these can be hand-made by twisting a metal thread around a drawing pin (Figure 2e).

Photochemical reaction system (Figure 1): The complete system includes a photosensitizer, KL 1500 LCD (Carl Zeiss Microscopy LLC, http://www.zeiss.de/micro/) as a low-energy generator, filter, and extension for delivery of the green light.

200 µl sterilized filter pipets (USA scientific Inc, Ocala, FL)

Figure 2: Anesthetic and surgical equipment. (a) Overview of the surgical area. (b) Anesthesia system: oxygen and isoflurane flow to induction chamber, mask and ventilator. (c) Dissecting microscope, heating pad on surgery panel, and ventilator. The anesthesia mask is attached to the panel. (d) Dry sterilizer. (e) Surgical tools, muscle retractors, and insulin syringe with rose bengal solution. (f) Rodent ventilator.

Suture materials with needle: 6-0 silk (Syneture) and 6-0 prolene (Ethicon Inc, cat. no. 8889H).

In vivo micro-CT (eXplore Vision CT 120, Trifoil Imaging): the equipment includes a micro-CT scanner, X-ray generator, a workstation for imaging acquisition and procession, anesthesia units (gas flow meter and isoflurane vaporizer), an EKG monitor, and a heating pad.

Accusync 71 electrocardiogram (ECG) trigger monitor (AccuSync Medical Research Corporation, MILFORD, CT)

EKG leads: carbon wire (Green 040IAX50FT, World Precision Instruments, Inc, Sarasota, FL)

Harvard pump 11 Plus Single Syringe (Harvard apparatus, www.harvardapparatus.com)

BioVet heating unit, Imaging Compatible (m2m Imaging Corp, www.m2mimaging.com)

Specimen micro-CT (eXplore Locus S, Trifoil Imaging)

AW workstation (Version 4.4, GE healthcare)

ImageJ software [freely available from the US National Institutes of Health (NIH)].

Procedure

Anesthesia: Timing 10-15 min

1. Clean the surgical area before use (Figure 2a-c). Sterilize surgical tools with Germinator 500 glass bead sterilizer beforehand (Figure 2d).
2. Set up the Leica MI6 stereo microscope and temperature-controlled surgical heating pad (Figure 2a-c).
3. Place the mouse into the anesthesia chamber.
4. Fill the chamber with 2% isoflurane inhalant in O_2 at a flow rate of 1.0-2 L/min from a metal vaporizer. Allows for fast recovery of mice under isoflurane anesthesia (Figure 2b).
5. Transfer the animal from the chamber onto a 37°C surgical heating pad once the mouse becomes unconscious (usually within several min). Place the animal in a supine position with the mouth covered by a mask with 2% isoflurane. Fix the mouse hands and feet with adhesive tape onto the pad and protect the mouse's eyes with puralube ophthalmic ointment.

Δ Critical Step: The depth of anesthesia is verified by foot pinches. If the mice are adequately anesthetized, there is no response from the extremity (flexion or withdrawal) (Figure 3a).

Coronary MVD Surgery: Timing 30-40 min

6. Make fresh 10 mg/ml rose bengal and stile extension of illumination as described before.
7. Briefly apply the Nair hair removing cream in the front neck and chest. Remove hair entirely from the surgical area. Clean residual cream with a warm water-soaked gauze and prepare the surgical field by gently scrubbing with betadine and 70% alcohol prep pads three times (Figure 3b-d).
8. Make a longitudinal cutaneous incision (approximately 7-8 mm) at the neck along the midline using iridectomy scissors and dumont curved tip serrated forceps (Figure 3e).
9. Expose the trachea with two home-made muscle retractors. Introduce an intubation cannula into the trachea through the mouth without tracheal incision under dissecting microscopic guidance (Figure 3g-h). Connect the cannula to a Harvard rodent ventilator preset at 2% isoflurane inhalant at a respiratory rate of 120 breaths per min (250 ul per breath) (Figure 2f). To drain the isoflurane, connect the exit of the ventilator machine to the air drainer.

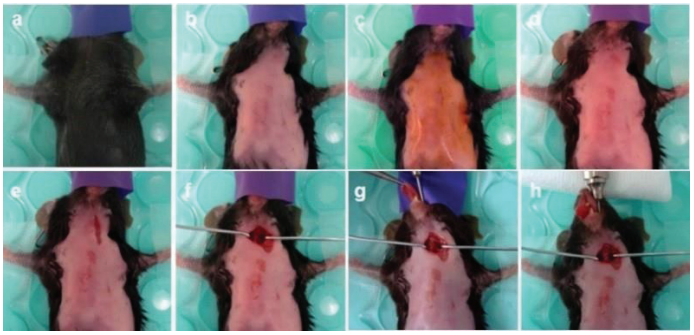

Figure 3: Intubation techniques. A mini-invasive technique via mouth approach is shown without tracheal incision. (a) Position of the mouse in the anesthesia mask on the heating pad. (b) Hair removal with Nair lotion. (c-d) Sterilizing the neck and the front chest wall with Betadine and 70% alcohol three times. (e) Incision of the skin. (f) Exposure of the trachea with two muscle retractors. (g) Introduction of an intubation cannula into the mouth. (h) Intubation under dissecting microscopic guidance, connection of cannula with a ventilator machine, and securing the system.

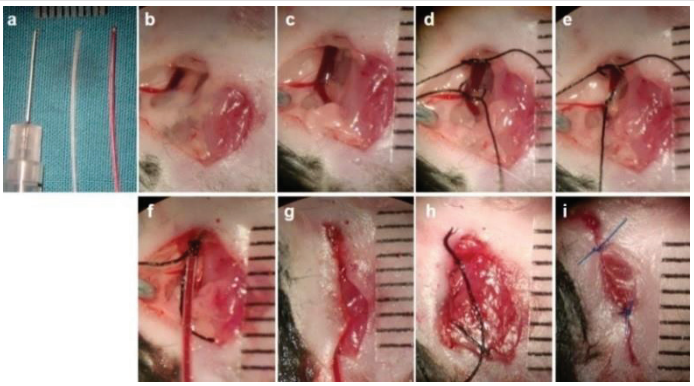

Figure 4: Jugular vein catheterization. A PE10 catheter is selected for catheterization using the same incision for tracheal intubation. (a) Preparation: insulin syringe with attached 29G needle (bend tip), PE 10 tube with and without rose bengal (photosensitizer). (b) Exposure of the left jugular vein. (c) Dissection of the left jugular vein. (d) 6-0 silk suture loop of the vein. (e) Ligation of distal suture. (f) Catheterization of a PE10 tube into the jugular vein under the help of a bend tip of an insulin syringe and a dissecting microscope. (g) Temporary closure of the incision. (h) Removal of the PE10 tube after photochemical induction in the heart. (i) Closure of the incision with a 6-0 prolene suture.

Δ Critical Step: It is important to do this step quickly so that the animal does not regain consciousness during intubation. Avoid injury to the trachea and the carotid artery.

10. Expose the left jugular vein and cannulate with a polyethylene catheter PE 10 for rose bengal infusion under microscopic guidance. Secure the catheter to the skin with a 6-0 silk suture (Figure 4a-i).

11. Make a longitudinal 6-8 mm incision down the center of the sternum to expose the underlying subcutaneous tissue at the front chest using an iridectomy scissors and dumont curved tip serrated forceps (Figure 5a).

12. Retract the pectoral muscles (Figure 5b). Penetrate the intercostal muscle with iridectomy scissors at the 4th intercostal space (Figure 5c). Apply the surgical cautery to the intercostal muscles to stop bleeding if necessary. Expose the edge of the left atria and the middle part of the heart. Place three home-made retractors to spread the ribs apart such that the heart is in view. Provide better visualization of the heart via widening of the incision site. Then dissect the pericardial membrane.

Δ Critical Step: The cautery shall only be used to stop bleeding in the muscular tissue where the medial incision is made. Be careful not to apply the cautery to any internal organs. To maximize animal recovery, the smaller the incision, the better for recovery.

13. Look for the superficial landmarks of the LAD course. The LAD cannot be visualized from the epicardium in mice because of its intramyocardial course, small diameter, and similar color to the background (Figure 6a,b). Instead, the last three branches of the coronary sinus vein are better used as superficial landmarks for our targeted region (Figure 6b-f).

Δ Critical Step: The middle part of the LAD and its surrounding microvasculature are targeted. To verify that our optimal parameters of PCR (4 min illumination combining with 10 mg/ml rose bengal) only induces endothelial dysfunction and microthrombi on the arteriole level, not at the epicardial coronary, we target both macro and micro-circulation. At the same time, a precise target is extremely important for us to avoid possible venous thrombosis in the coronary sinus, which may confound molecular imaging results. For illustrative purposes, the heart was exposed widely; 0.1 ml 2% Evans blue was injected into the jugular vein to highlight the coronary sinus; and 50 µl 10% bismuth nanoparticle was perfused via a PE 10 tube into the coronary arterial system to highlight the LAD and its branches. The spatial relationship among our target, the sinus vein branches, and the LAD can thus be clarified (Figure 6c).

14. Inject slowly 0.1 ml 10 mg/ml rose bengal through the previously inserted PE10 catheter (Figure 5c). After administration of rose bengal, the heart and surrounding lung tissue gains a pinkish color.

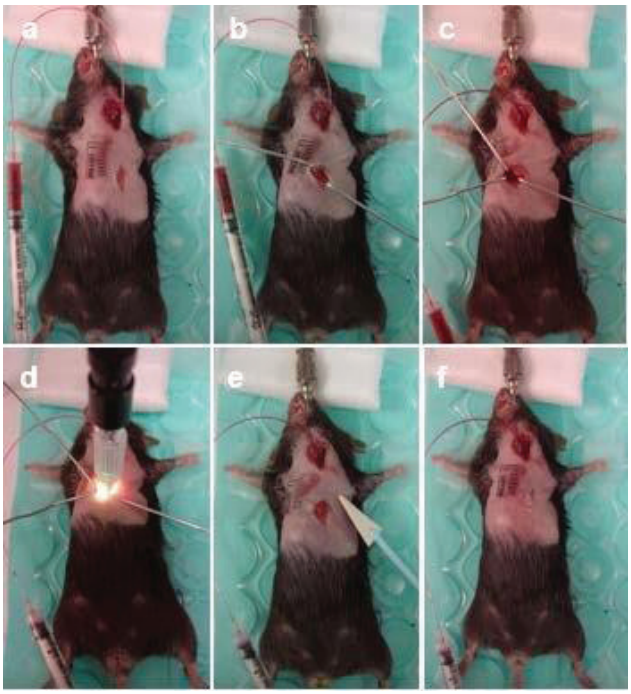

Figure 5: PCR-induced coronary MVD. (a) Position the mouse same as tracheal intubation and create a skin incision in the front of chest down the center of the sternum. (b) The pectoral muscles are retracted. (c) The intercostal muscle is penetrated and retracted to expose the heart surface. (d) Using the sinus branches as landmarks to locate the middle portion of the LAD, focal photochemical reaction is induced for 4 min 1 min after injection of 0.1 ml 10mg/ml rose bengal. (e) Absorb the fluid inside the left chest with a cotton-tipped applicator and inflate the lung. (f) Use two sutures with a 6-0 prolene to close the intercostal space (thoracotomy), and an additional two stitches to close the thoracic incision.

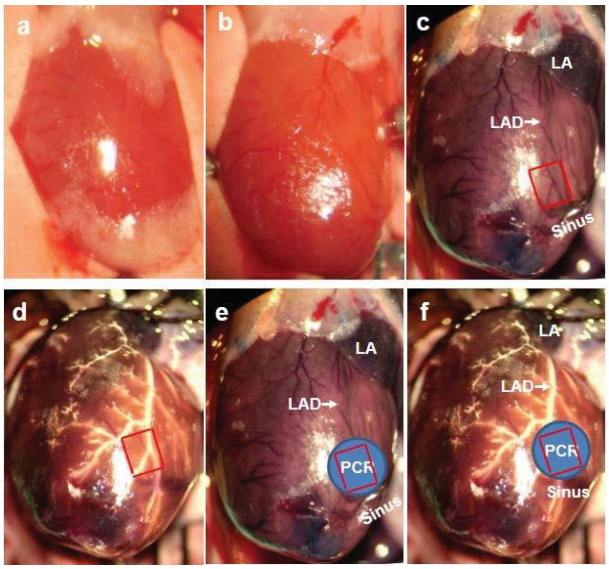

Figure 6: Coronary sinus branches as landmarks of the middle portion of the LAD for PCR. (a) Open chest to expose the heart and intact pericardium. (b) Dissect the pericardium to expose clearly the surface of the heart. Every visible vessel is a vein. (c) 2% Evans blue is injected into the left jugular vein and circulated for 1 minute only in this case. Evans blue highlights both coronary sinus system and the coronary artery. The LAD is visible. The last three branches of the sinus are used as landmarks for the LAD. 1 mm x 1 mm square area in red is superposed on these branches. (d) To further highlight the LAD for spatial relationships between the coronary artery and sinus branches, 20% bismuth oxychloride nanoparticle in 5% gelatin is injected into the ascending aorta to fill the coronary arterial system. 1 mm x 1 mm square area in red is superposed on the middle portion of the LAD. (e) 2 mm diameter blue region is superimposed on (c) to show our targeting region for PCR. (f) 2 mm diameter blue region is superimposed on (d) to show our targeting region for PCR. Scale bar is 1 mm.

15. Position a 2 mm diameter tip of KL1500 LCD cold light beam with 540nm wavelength in the targeted region onto the heart surface (Figure 6c-f). Turn on the green light to induce focal photochemical reaction 1 min after rose bengal is injected (Figure 5d). Illuminate the heart for 4 minutes.

Δ Critical Step: A timer should be used to record the initiating time and the ending time to calculate PCR time (4 minutes) 1 min after administration of 0.1 ml 10 mg/ml rose bengal.

During PCR, animals will experience a slower heart rate without arrhythmia or ST-segmental elevation, which can be observed from the EKG. EKG signals are normal 10 min after the procedure in our preliminary study.

The duration of PCR will determine the severity and size of the infarct-let and the vascular response. We have found that 4 min is sufficient to produce an infarct-let size of 5-7% without the spasm of the LAD. We have successfully induced reproducible arteriole occlusions and infarct-let using these parameters.

Troubleshooting (Table 1)

16. Clean the chest cavity with a cotton-tipped applicator and inflate the lung with temporary blockage of the exit of air flow (Figure 5e).

17. Draw together the rib cage and close the intercostal space with two single 6-0 prolene suture knots, Dumont curved tip serrated forceps and a needle holder.

18. Spray betadine on a piece of gauze and wipe along the suture site. Close the chest skin incision with an additional 2 stitches of 6-0 prolene sutures at approximately 3mm between sutures (Figure 5f).

19. Withdraw the intra-jugular PE10 catheter and suture the neck incision with 6-0 prolene.

20. Receive rose bengal injection only, illumination only, or neither of them (sham-operation) in control mice.

21. Wan off aesthesia after surgical procedures, while keeping mice warm on a temperature-controlled pad, monitoring animal movements. Once the animal shows signs of movement, remove the animal from the ventilator. Return the mouse back into its original cage with free access to food and water in a temperature-controlled room with 12-hour light and dark cycles. Monitor frequently until mice recover to normal activities (usually 30 min later).

Δ Critical Step: The duration that the animal is allowed to recover before imaging or therapy will determine the type of MVD model. For an acute model, the injured heart experiences endothelial dysfunction, acute microthrombi, and early ischemia. The early detection or treatment should be performed within the first couple of hours. For a chronic model, the heart undergoes infarct and fibrosis secondary to the penetration of inflammatory cells and long-term ischemia.

22. Administer a single dose of buprenorphine (0.1 mg/ml) subcutaneously to control ischemic pain and administer cephalexan (25 mg/kg) intramuscular injection to minimize infection.

If you perform coronary MVD successfully, microvascular occlusion at the arteriole level with preserved left ventricle function can be confirmed by measuring cardiac function with *in vivo* cardiac gating CT after PCR (Figure 8), and by confirming rarefaction via high-resolution micro-CT coronary angiogram (Figure 6f, Figure 7f), which shows the distribution of both macro- and microvasculature. If desired, proceed to option A or option B.

A. *in vivo* micro-CT to confirm the preserved cardiac function: Timing 20-30 min.

The eXplore Vision 120 CT can perform prospectively-gated cardiac imaging with high precision to reduce motion artifacts in the heart and thorax. Features of this equipment include rapid scans facilitated by a 5 kW pulsed high-output x-ray tube, application flexibility enabled by adjustable imaging parameters (tube potential 70-120 kV, current up to 50 mA, and exposure time as short as 8ms), rodent cardiac imaging made possible by less than 1 milli-second pulse precision that is capable of capturing over 600 beats per minute, and multi-modality support built-in for hybrid imaging and x-ray filtering which reduces animal dose and decreases image artifacts.

Table 1: Troubleshooting table.

Step	problem	Possible reason	Solution
15	Various locations of MVD	Landmark is wrong	Use coronary sinus & its last three main branches as landmarks
15	Various sizes of MVD	Tip of light extension moves during PCR	Gently push the tip against the heart surface
15	Epicardial coronary spasm	Illumination time may be too long	Shorten the illumination time.
15	Animals die after thoracotomy and MVD induction at a high-mortality rate	The concentrations of rose Bengal is too high and illuminating time too long.	Reduce the concentration of rose bengal and shorten the illumination time
27	*In vivo* cardiac gated microCT fails	Heart rates change more than 15%	Keep the heart rates stable with proper isoflurane and a BioVet heating pad
30	Coronary angiogram shows oronary hypo-perfusion	Heart does not rest at the diastolic phase	Saturated KCL to rest the heart at the end of the diastolic state
36	Coronary angiogram fails	No proper coronary perfusion; no good ontrast agents	Retrograde cannulation into the ascending aorta without leakage; use heavy metal nanoparticle to enhance radiopaque due to the

Δ Critical Step: Avoid motion artifacts because of twitching. Keep the depth of anesthesia sufficient.

Cardiac gated imaging of mice poses a challenge to the researcher because of the relatively small size of the animals and the high respiratory and cardiac frequencies. At rest, the heart rate of mice ranges between 400 and 600 beats per minute (bpm), and the breathing frequency of mice is about 200. The application of gating strategies is necessary to achieve high resolution imaging of heart structures *in vivo*.

Prospective gating is already implemented in most micro-CT systems.

23. Position the anesthetized mice prone on the custom-made mouse bed.

24. Breathe freely throughout the experiment.

25. Obtain the ECG signals from affixing three ECG electrodes to two forepaws and one hind limb of the animal using an Accusync 71 monitor. The cardiac trigger points are set at peaks of the R waves in the ECG presented graphically in Figure 8b.

Δ Critical Step: The first R wave occurring within the acquisition window generates a software trigger point for phase 1, from which the subsequent triggers are derived after a user-definable delay based on the heart rate. This user-definable delay is the time delay after the R peak, which is used to select the desired imaging phases in the cardiac cycle (8 phases in this study). To minimize the variation and motion artifact, the animal should be kept warm and heart rate should remain stable.

26. Administer eXia 160, a blood-pool contrast agent intravenously in a single bolus at a dose of 5 µl/g bodyweight as recommended by the manufacturer, prior to *in vivo* micro-CT imaging.

Note: This iodinated contrast agent has been shown to provide significant enhancement of the mouse vasculature (up to 500 HU for up to 30 min) after injection [32]. Because of this long retention time, it is possible to acquire multiple cardiac micro-CT data sets from the same mouse after injection. Due to its enhancement in the myocardium [32], it is also possible to acquire cardiac viability data sets from the same mouse 2-24 hours after injection.

27. Acquire images. The micro-CT scanner is operated with 80-kVp x-ray tube voltage, 32-mA tube current, 16-millisecond exposure time per frame, 4 × 4 detector binning model, 220°, and 20 offsets. This acquisition resulted in an 8-phase set of contiguous images through the entire heart. These images can be reconstructed as isotropic 100×100×100 pixels with a voxel size of 98µm. All reconstructions are done with a Feldkamp algorithm and all images are calibrated with standard Hounsfield units (HU) using micro View.

Troubleshooting (Table 1)

28. Analyze the images by transferring the reconstructed cardiac images to a AW workstation and measuring the cardiac function by contouring the left ventricle at different phases for end-diastolic volume, end-systolic volume, and ejection fraction.

Δ Critical Step: One concern of *in vivo* cardiac micro-CT is its radiation dosage. For acquiring one volumetric data set, the entrance dose is calculated to be 10 cGy using our proposed protocol, which is similar to the dose delivered by a clinical multi-slice CT scanner (8-11 cGy) [33]. No adverse effects due to radiation are observed in mice over the period of 4 weeks in our work.

B. Postmortem high-resolution micro-CT angiogram and imaing reconstruction [34-36]: Timing 4.5-5.5 h: Timing 10-15 min.

29. Heparinize intraperitoneally the animal for 1 min with 100 IU heparin.

30. Euthanize the animals and rest the heart at the end of diastolic phase with saturated KCL at selected time points.

Troubleshooting (Table 1)

31. Place the euthanized animal in a supine position.

32. Make an incision from the abdominal muscles to the top of the rib cage.

33. Catheterize a tampered PE10 tube into the ascending aorta, right above the ostium of the coronary arteries, and secure the tube with a 6-0 silk suture.

Δ Critical Step: Flare the tip of the PE10 tube and make it bigger, however, make sure the lumen is the same size as the normal tube.

34. Rinse away blood from the coronary with 0.5 ml saline via the PE 10 tube under 100 mmHg pressure. Cut the IVC as outflow.

35. Infuse 0.5 ml 2% paraformaldehyde (PFA) in saline under the same pressure.

36. Inject 0.05-0.1 ml 20% bismuth nanoparticle (in 5% gelatin) via the PE10 tube. Under microscopic guidance, once the contrast agent reaches the apex, cover the heart with wet iced cold water for at least 30 min to polarize the contrast agent.

Δ Critical Step: Take advantage of the sizes of our bismuth nanoparticles (~300 nm diameter), since the cluster of these nanoparticles is hard to reach the coronary sinus. To further make sure contamination from the venous system is limited, the contrast agent can be stop with iced water because it contains 5% gelatin (transfer from liquid at room temperature to the solid at 4°C).

Troubleshooting (Table 1)

37. Excise the heart and place the heart into a 1.5 ml vial containing 2% PFA overnight, prior to micro-CT imaging.

38. Dry the heart with paper and fill the bi-ventricles with ultrasound gel.

39. Scan the arterial vasculature in the heart with a specimen micro-CT imaging scanner with a cone beam filtered back projection algorithm, set to a 0.008-mm effective detector pixel size. Micro-CT is operated with 60-kVp x-ray tube voltage, 100-mA tube current, 2960-milli-second per frame, 1 × 1 detector binning model, 360°, and 0.5° increments per view. This acquisition results in a set of contiguous VFF-formatted images through the entire heart.

40. Calibrate vff image data in standardized Hounsfield (HU) for quantitative analysis with MicroViewTM software.

41. Transfer the calibrated images to AW 4.4 workstation for volume render and multiple format reconstruction.

42. Calculate the vascular size distribution with NIH imaging.

Timing

Steps 1–5, anesthesia: 10-15 min.

Steps 6, preparation of fresh photosensitizer extension of the light probe: 5-10 min.

Steps 7-22, coronary MVD model: approximately 30-40 min.

Steps 23–28, *in vivo* cardiac gated micro-CT: 15-20 min scan time and 5-10 min for reconstruction.

Steps 29-40, specimen micro-CT coronary angiogram: 4-5 h scan time depending on spatial resolution.

Steps 41-42, specimen micro-CT imaging reconstruction and quantitative analysis: 30 min.

Anticipated results

To develop a reproducible mouse model of coronary MVD with similar features to clinical MVD patients, we have established a PCR-based approach in the mouse heart. After successful PCR, the illuminated zone becomes discolored, a reddish patch that can be superficially visible even at the early stage, and a white patch as ischemia, infarct-let, or fibrosis at the late stage (day 7 or after). At the early stage (24 hours after PCR), EM should show endothelial dysfunction, broken cell-cell junction, and leakage of blood components at the arterioles (Figure 7d). Fluorescent coronary angiogram should show no-flow zone in the anterolateral wall supplied by the LAD branches (Figure 7b). At the late stage (day 14), high-resolution microCT angiogram should show less arterioles within PCR-treated region with patent epicardial coronary arteries (Figure 7f), which indicates pre-capillary arteriole occlusion. Histology should demonstrate peri-arteriole fibrosis (Figure 7h).

We have an overall surgical success rate of over 92% (107 of 116 mice) using this model based on the histological analysis of ischemic lesions and molecular imaging results (gamma-well counting results). The mortality rate within 7 days after MVD is <6% (6 of 110 mice). Accidental fatalities will occur either immediately after PCR or within 24 hours of recovery. Sham-operated control mice with light only, photosensitizer only, or nothing, do not show any microvascular occlusion or ischemic lesions.

PCR applied on the coronary microcirculation should induce ROS over-production, specifically singlet oxygen. Immunohistochemical techniques may be used to document ROS type in the anterior wall [7]. Evidence has suggested that patients' gender may play a role in primary MVD, therefore, we only use female mice in the current study. Additionally,

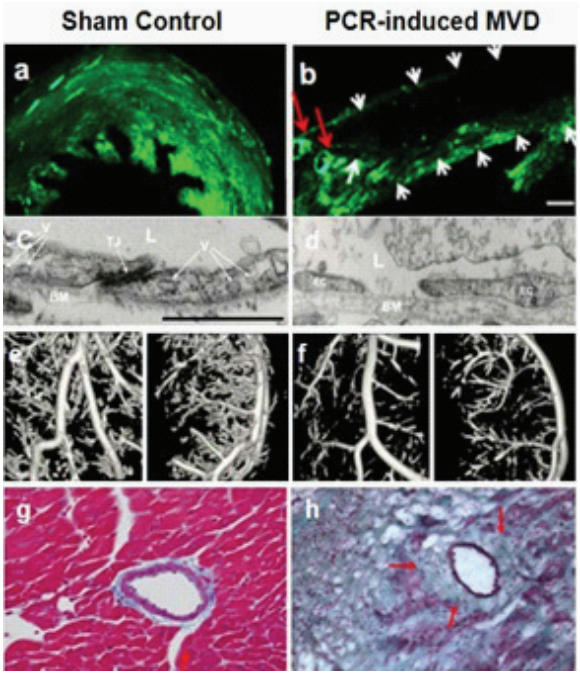

Figure 7: Coronary fluorescent angiogram, scanning electron microscopy (EM) images, micro- CT angiogram, and histology in the sham control (a, c, e, g) and PCR-induced MVD (b, d, f, h) mice. (a-b) Confocal microscopic images of 60 um-axial heart sections from control or PCR- induced MVD mice subjected to FITC-dextran (green) injection revealed normal perfusion (a), or "no-flow" zone in the MVD region with preserved fluorescent signal within the large epicardial coronaries (b) at 24 hours after MVD-induction. Red arrows indicate the LAD branches and white arrows indicate the border of the PCR-induced MVD. Scale bar is 170 μm. (c-d) EM images show that 24h-old MVD with endothelial dysfunction, broken cell-cell junction, and leakage of the blood components including fibrin and a few RBCs (d), compared to normal endothelial cells and tight junction (c). Adapted with permission from Zhuang et al. [7]. Scale bar is 1 μm. (e-f) Coronary micro-CT angiogram with bismuth-oxychloride-gelatin shows focal rarefaction of the coronary branches within a chronical MVD lesion 14 days post-MVD induction (f), as well as its control (e), which indicates occluded arterioles with patent LAD and main branches. Spatial resolution is 14 μm. (g-h) Histology with trichrome staining shows normal arterioles with healthy myocardium in the control mouse (g), and peri-arteriole fibrosis surrounded by infarct-let in a chronic MVD lesion (h) (14 days) (×200).

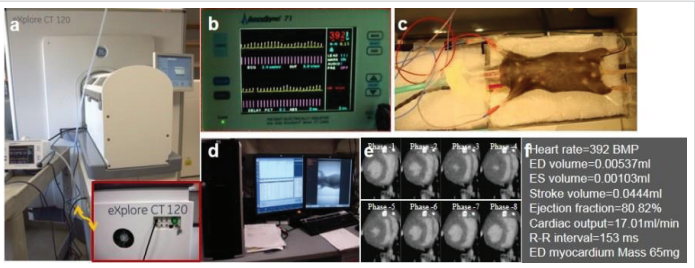

Figure 8: *In vivo* micro-CT imaging. (a) Overview of micro-CT scanner. Inset: a cardiac gating trigger unit with a connecting cable from an EKG monitor. (b) An EKG monitor with appropriate heart frequency signals in yellow and triggering markers in red. (c) Mouse on the heat pad, EKG leads, anesthesia mask and connection of the anesthesia to the container. (d) Computer screen with built-in software for acquisition, reconstruction, and transferring to another workstation for further reconstruction and quantification. (e) Representative 8 phases cardiac micro-CT showing circumference of the endocardial and epicardial wall after contrast agent is administrated. (f) Direct measurement and calculation of results from in vivo cardiac micro-CT scan. Note: Red dots on yellow ECG waveforms show R-Peak detection; red lines show trigger prescription.

to have enough tissue samples post-intervention for the evaluation of protein levels and gene expressions, we apply a 2 mm tip of extension for light delivery, and subsequently induced a slight ischemic region. In fact, we can modify the tip size for a smaller lesion as well. It is important to be aware that the size of MVD is adjustable, and depending on the purposes of the study, researchers can consider inducing multiple small lesions instead of single large lesion.

The technique employed to establish a model of coronary MVD involves the combination of a photosensitizer (rose bengal) and low energy light. Once this photosensitizer is absorbed by endothelial cells and other cells, including myocytes, focal illumination of the interest area will activate the photosensitizer. This action subsequently damages these cells by over-producing oxidative stress, opening the endothelial barrier, activating platelets, recruiting factor XIII to cross-link fibrin, and inducing microthrombi [7].

With the current *in vivo* micro-CT scanning protocol, the average data acquisition time for one 8-phase cardiac gated scan is about 12-16 min. The scanning time depends on the heart rate based on EKG readings. The calculated cardiac functions, based on these cardiac gated images, show mild non-significant decrease (Figure 8e,8f), which means that cardiac function is preserved in coronary MVD model over time. In other words, this commonly used imaging modality is not sensitive enough to reliably detect cardiac function subsequent to photochemically-induced MVD. In our model, cardiac dysfunction is not evident for at least two weeks. Coronary micro-CT angiography clearly demonstrate normal macro and micro-vasculature in a control mouse (Figure 7e), and only microvascular rarefaction in the region of illumination without change of macro-vasculature in a mouse with PCR.

In conclusion, the mouse model of coronary MVD presented here enables researchers to mimic the clinical events of this disease. The presence of *in situ* PCR on the heart surface produces repeatable micro-thrombi in the coronary arterioles, local ischemia, infarct-let, and perivascular fibrosis, with preserved cardiac function. We believe that our model will be helpful to assist the molecular probe in early diagnosis, screen therapeutic drugs that have the potential to prevent diseases progression, evaluate potential interventions, and to investigate the complex pathophysiology of this disease.

Acknowledgment

This work was supported by National Institutes of Health grant 5R21HL119975 and P01HL107205 (Imaging Core) (Z.W.Z).

Author's contributions

ZZW contributed to conception and design and revised the manuscript, carried out the experiments and drafted the manuscript. ZZW, XW, and FL carried out the experiments. All author read and approved the final manuscript.

References

1. Shaw LJ, Merz CN, Pepine CJ, Reis SE, Bittner V, et al. Women's Ischemia Syndrome Evaluation (WISE) Investigators. The economic burden of angina in women with suspected ischemic heart disease: results from the National Institutes of Health--National Heart, Lung, and Blood Institute--sponsored Women's Ischemia Syndrome Evaluation. Circulation. 2006; 114: 894-904.
PubMed: https://www.ncbi.nlm.nih.gov/pubmed/16923752

2. Reis SE, Holubkov R, Conrad Smith AJ, Kelsey SF, Sharaf BL, et al. WISE Investigators. Coronary microvascular dysfunction is highly prevalent in women with chest pain in the absence of coronary artery disease: results from the NHLBI WISE study. Am Heart J. 2001; 141: 735-741.
PubMed: https://www.ncbi.nlm.nih.gov/pubmed/11320360

3. Pepine CJ, Anderson RD, Sharaf BL, Reis SE, Smith KM, et al. Coronary microvascular reactivity to adenosine predicts adverse outcome in women evaluated for suspected ischemia results from the National Heart, Lung and Blood Institute WISE (Women's Ischemia Syndrome Evaluation) study. J Am Coll Cardiol. 2010; 55: 2825-2832.
PubMed: https://www.ncbi.nlm.nih.gov/pubmed/20579539

4. Likoff W, Segal BL, Kasparian H. Paradox of normal selective coronary arteriograms in patients considered to have unmistakable coronary heart disease. N Engl J Med. 1967; 276: 1063-1066.
PubMed: https://www.ncbi.nlm.nih.gov/pubmed/6025663

5. Mosseri M, Yarom R, Gotsman M, Hasin Y. Histologic evidence for small-vessel coronary artery disease in patients with angina pectoris and patent large coronary arteries. Circulation. 1986; 74: 964-972.
PubMed: https://www.ncbi.nlm.nih.gov/pubmed/3769180

6. Suzuki H, Takeyama Y, Koba S, Suwa Y, Katagiri T. Small vessel pathology and coronary hemodynamics in patients with microvascular angina. Int J Cardiol. 1994; 43: 139-150.
PubMed: https://www.ncbi.nlm.nih.gov/pubmed/8181868

7. Zhuang ZW, Huang Y, Ju R, Maxfield MW, Ren Y, et al. Molecular imaging of factor XIII activity for the early detection of mouse coronary microvascular disease. Theranostics. 2019; 9: 1474-1489.
PubMed: https://www.ncbi.nlm.nih.gov/pubmed/30867844

8. Granger D, Rodrigues S, Yildirim A, Senchenkova E. Microvascular responses to cardiovascular risk factors. Microcirculation. 2010; 17: 192-205.
PubMed: https://www.ncbi.nlm.nih.gov/pubmed/20374483

9. Shaw LJ, Bairey Merz CN, Pepine CJ, Reis SE, Bittner V, et al. Insights

from the NHLBI- Sponsored Women's Ischemia Syndrome Evaluation (WISE) Study: Part I: gender differences in traditional and novel risk factors, symptom evaluation, and gender-optimized diagnostic strategies. J Am Coll Cardiol. 2006; 47(3 Suppl): S4-S20.
PubMed: https://www.ncbi.nlm.nih.gov/pubmed/16458170

10. Pepine CJ, Kerensky RA, Lambert CR, Smith KM, von Mering GO, et al. Some thoughts on the vasculopathy of women with ischemic heart disease. J Am Coll Cardiol. 2006; 47(3 Suppl): S30-35.
PubMed: https://www.ncbi.nlm.nih.gov/pubmed/16458168

11. Kaski JC, Aldama G, Cosín-Sales J. Cardiac syndrome X. Diagnosis, pathogenesis and management. Am J Cardiovasc Drugs. 2004; 4: 179-194.
PubMed: https://www.ncbi.nlm.nih.gov/pubmed/15134470

12. Versari D, Daghini E, Virdis A, Ghiadoni L, Taddei S. Endothelial Dysfunction as a Target for Prevention of Cardiovascular Disease. Diabetes Care. 2009; 32: S314-S321.
PubMed: https://www.ncbi.nlm.nih.gov/pubmed/19875572

13. Cai H, Harrison DG. Endothelial dysfunction in cardiovascular disease: the role of oxidant stress. Circ Res. 2000; 87: 840-844.
PubMed: https://www.ncbi.nlm.nih.gov/pubmed/11073878

14. Egashira K, Hirooka Y, Kuga T, Mohri M, Takeshita A. Effects of L-arginine supplementation on endothelium-dependent coronary vasodilatation in patients with angina pectoris and normal coronary arteriograms. Circulation. 1996; 94: 130-134.
PubMed: https://www.ncbi.nlm.nih.gov/pubmed/8674170

15. Tousoulis D, Briasoulis A, Papageorgiou N, Tsioufis C, Tsiamis E, et al. Oxidative Stress and Endothelial Function: Therapeutic Interventions. Recent Pat Cardiovasc Drug Discov. 2011; 6: 103-114.
PubMed: https://www.ncbi.nlm.nih.gov/pubmed/21513492

16. Pennathur S, Heinecke JW. Oxidative stress and endothelial dysfunction in vascular disease. Curr Diab Rep. 2007; 7: 257-264.
PubMed: https://www.ncbi.nlm.nih.gov/pubmed/17686400

17. Griendling KK, Sorescu D, Ushio-Fukai M. NAD(P)H oxidase: role in cardiovascular biology and disease. Circ Res. 2000; 86: 494-501.
PubMed: https://www.ncbi.nlm.nih.gov/pubmed/10720409

18. Madamanchi NR, Runge MS. Mitochondrial dysfunction in atherosclerosis. Circ Res. 2007; 100: 460-473.
PubMed: https://www.ncbi.nlm.nih.gov/pubmed/17332437

19. Caccese D, Pratico D, Ghiselli A, Natoli S, Pignatelli P, et al. Superoxide anion and hydroxyl radical release by collagen-induced platelet aggregation: role of arachidonic acid metabolism. Thromb Haemost. 2000; 83: 485-490.
PubMed: https://www.ncbi.nlm.nih.gov/pubmed/10744158

20. Maki J, Hirano M, Hoka S, Kanaide H, Hirano K. Involvement of reactive oxygen species in thrombin-induced pulmonary vasoconstriction. Am J Respir Crit Care Med. 2010; 182: 1435-1444.
PubMed: https://www.ncbi.nlm.nih.gov/pubmed/20639439

21. Zhuang ZW, Shi J, Rhodes JM, Tsapakos MJ, Simons M. Challenging the surgical rodent hindlimb ischemia model with the miniinterventional technique. J Vasc Interv Radiol. 2011; 22: 1437-1446.
PubMed: https://www.ncbi.nlm.nih.gov/pubmed/21459613

22. Nichols TC, Bellinger DA, Reddick RL, Read MS, Koch GG, et al. Role of von Willebrand factor in arterial thrombosis: studies in normal and von Willebrand disease pigs. Circulation. 1991; 83: IV56-IV64.
PubMed: https://www.ncbi.nlm.nih.gov/pubmed/2040072

23. Malyar NM, Lerman LO, Gössl M, Beighley PE, Ritman EL. Relationship between Surface Area of Nonperfused Myocardium and Extravascular Extraction of Contrast Agent following Coronary Microembolization. Am J Physiol Regul Integr Comp Physiol. 2011; 301: R430-R437.
PubMed: https://www.ncbi.nlm.nih.gov/pubmed/21543631

24. Li L, Li DH, Qu N, Wen WM, Huang WQ. The role of ERK1/2 signaling pathway in coronary microembolization-induced rat myocardial inflammation and injury. Cardiology. 2010; 117: 207-215.
PubMed: https://www.ncbi.nlm.nih.gov/pubmed/21150201

25. Carlsson M, Wilson M, Martin AJ, Saeed M. Myocardial microinfarction after coronary microembolization in swine: MR imaging characterization. Radiology. 2009; 250: 703-713.
PubMed: https://www.ncbi.nlm.nih.gov/pubmed/19164123

26. Falk E. Unstable angina with fatal outcome: dynamic coronary thrombosis leading to infarction and/or sudden death: autopsy evidence of recurrent mural thrombosis with peripheral embolization culminating in total vascular occlusion. Circulation. 1985; 71: 699-708.
PubMed: https://www.ncbi.nlm.nih.gov/pubmed/3971539

27. Li SM, Zeng K, Wang WW, Zhang FL, Sun XD, et al. Time course of myocardial NF-kappaB activation post coronary microembolization. Zhonghua Xin Xue Guan Bing Za Zhi. 2008; 36: 1016-1020.
PubMed: https://www.ncbi.nlm.nih.gov/pubmed/19102917

28. Haft JI, Kranz PD, Albert FJ, Fani K. Intravascular platelet aggregation in the heart induced by norepinephrine. Circulation. 1972; 46: 698-708.
PubMed: https://www.ncbi.nlm.nih.gov/pubmed/5072771

29. Ciulla MM, Paliotti R, Ferrero S, Braidotti P, Esposito A, et al. Left ventricular remodeling after experimental myocardial cryoinjury in rats. J Surg Res. 2004; 116: 91-97.
PubMed: https://www.ncbi.nlm.nih.gov/pubmed/14732353

30. van Amerongen MJ, Harmsen MC, Petersen AH, Popa ER, van Luyn MJ. Cryoinjury: a model of myocardial regeneration. Cardiovascular Pathology. 2008; 17: 23-31.
PubMed: https://www.ncbi.nlm.nih.gov/pubmed/18160057

31. Dolmans D, Fukumura D, Jain RK. Photodynamic therapy for cancer. Nat Rev Cancer. 2003; 3: 380-387.
PubMed: https://www.ncbi.nlm.nih.gov/pubmed/12724736

32. Detombe SA, Dunmore-Buyze J, Drangova M. Evaluation of eXIA 160 cardiac-related enhancement in C57BL/6 and BALB/c mice using micro-CT. Contrast Media Mol Imaging. 2012; 7: 240-246.
PubMed: https://www.ncbi.nlm.nih.gov/pubmed/22434637

33. Morin RL, Gerber TC, McCollough CH. Radiation dose in computed tomography of the heart. Circulation. 2013; 107: 917-922.
PubMed: https://www.ncbi.nlm.nih.gov/pubmed/12591765

34. Hofmann JJ, Briot A, Enciso J, Zovein AC, Ren S, et al. Endothelial deletion of murine Jag1 leads to valve calcification and congenital heart defects associated with Alagille syndrome. Development. 2012; 139: 4449-4460.
PubMed: https://www.ncbi.nlm.nih.gov/pubmed/23095891

35. Landskroner-Eiger S, Qiu C, Perrotta P, Siragusa M, Lee MY, et al. Endothelial miR-17~92 cluster negatively regulates arteriogenesis via miRNA-19 repression of WNT signaling. Proc Natl Acad Sci USA. 2015; 112: 12812-12817.
PubMed: https://www.ncbi.nlm.nih.gov/pubmed/26417068

36. Kivelä R, Bry M, Robciuc MR, Räsänen M, Taavitsainen M, et al. VEGF-B-induced vascular growth leads to metabolic reprogramming and ischemia resistance in the heart. EMBO Mol Med. 2014; 6: 307-321.
PubMed: https://www.ncbi.nlm.nih.gov/pubmed/24448490